ISBN: 978-981-18-5852-9
WCSE 2022 Spring Event: 2022 9th International Conference on Industrial Engineering and Applications
doi: 10.18178/wcse.2022.04.020

Distributed Optimal Dispatch of Integrated Energy System Considering Privacy-Preserving

Han Zhang [1], Kun Huang [1], Zhenwei Zhang [2 +], Chengfu Wang [2], Rui Xu [1], Hao Wang [1], Zixian Ding [1], Yue Cui [1]

[1] Global Energy interconnection Group Co., Ltd. Beijing, China
[2] School of Electrical Engineering, Shandong University, Jinan, China

Abstract. To solve the problem of information privacy between integrated energy systems (IES) for unified operation, a cross-regional distributed coordination control strategy under incomplete information conditions is proposed. Firstly, the incomplete information conditions are explained based on the types and characteristics of cross-regional multi-energy coordination, and the coupling port can be used to exchange part of the information for multi-agent autonomous coordination. The implementation method adopts the alternating direction method of multipliers (ADMM) and optimizes iterative method. Secondly, combined with the principle of decentralized consistency, the ADMM global consistency framework is constructed, and the system is decomposed at inter-regional connection lines and pipelines in combination with boundary replication. Then, the objective function and constraint conditions are decomposed according to the region, and the convergence speed of the calculation process is further accelerated from the two aspects of model linearization and variable penalty parameters. Finally, the feasibility of the algorithm and the effectiveness of the proposed strategy are analyzed and verified with a simulation case.

Keywords: integrated energy system (IES), alternating direction method of multipliers (ADMM), distributed optimal dispatch, information privacy

1. Introduction

Since the concept of IES that integrates multiple types of heterogeneous energy from electricity, heat, and natural gas is put forward, it has faced the problem of overcomplicated coordination and control of multi-energy systems in the time and space dimensions. On the one hand, there are significant differences in the transmission characteristics of electricity, gas, and heat energy flow, and the dynamic processes of the network influence each other [1], which makes the coordination and control problem extremely complicated. On the other hand, although multi-energy systems are closely coupled in space, the isolation between different energy systems is still difficult to break. To protect the privacy of each energy area in the process of inter-regional energy transmission, there is a situation that information is not completely interoperable. Literature [2] pointed out that the realization of the coordinated optimization design of the entire process of electricity, gas, cooling, heat, and other energy sources is a key technical difficulty that needs to be solved urgently in the research of comprehensive energy systems. Literature [3] elaborated on the importance of coordinated regulation of an integrated energy system with multiple energy sources, multiple goals, and multiple variables in promoting the consumption of renewable energy. Literature [4] constructed an evaluation index system that considers the coordination and optimization of multi-energy systems, safety and stability, economic and social benefits.

The research of coordinated control methods for integrated energy systems can be divided into three types: centralized control, hierarchical control, and distributed control. The centralized control method treats various energy systems as a whole and requires a central server to collect all operating information. Literature [5] carried out a unified power flow calculation for a regionally integrated energy system coupled with electricity, gas, and heat, in which the thermal load was regarded as a given value to focus on the interaction between power and natural gas system networks. Literature [6] considers the uncertain factors at

+ Corresponding author. Tel.: 17854291192; *E-mail address*: 1529791303@qq.com.

both ends of the source and load, and further proposes a unified probability energy flow method. Literature [7] considers the compressibility of natural gas and establishes a mixed-integer linear programming model for electricity and gas interconnected systems. Literature [8] introduced P2G technology into collaborative planning to build a two-way coupling relationship between the power system and the natural gas system. The above-mentioned literature has researched the control theory of multi-energy systems based on centralized control methods, forming an early research framework for integrated energy systems.

To balance the relationship between multi-stakeholders and the need for regulation, the hierarchical regulation method is applied in the integrated energy system [9]. At present, the hierarchical control method still relies on the central server to communicate and coordinate between the upper and lower subjects. However, compared with the centralized control method, the interesting relationship between multiple energy subjects is clear, which is conducive to the implementation of multiple goals. Literature [10] pointed out that the development of a reasonable operating system and hierarchical control methods are conducive to ensuring the safe, stable, and economic operation of the power system, but it requires a complete and advanced communication network as support. Literature [11] considers the different interest demands of energy suppliers and users. Literature [12] constructs a regional IES bi-level planning method that takes into account the maximization of the net income of energy operators. Literature [13] implements hierarchical coordination control for the two periods of day and builds IES hierarchical coordination control architecture. Literature [14] proposed a hierarchical and distributed energy coordination scheme for IES with multi-agent systems. The hierarchical and distributed idea can effectively reduce the communication requirements between multi-level subjects.

The above two methods generally rely on a central server for information collection and coordination, and have high-performance requirements for communication systems and servers. For this reason, more and more researchers have begun to apply distributed algorithms to the research of integrated energy system operation control. Literature [15] summarized the current research objects of distributed optimization problems into two categories. Literature [16] pointed out that the consensus-based distributed optimization algorithm was an important foundation and development direction of distributed optimization research in the past few decades, and summarized two types of solution methods, primitive domain, and dual-domain. Distributed gradient [17] and dual average method [18], as typical primitive domain solving methods, have the characteristics of simple calculation and good robustness, but the above algorithms cannot take into account both convergence and calculation accuracy. The dual-domain solution rule represented by the dual ascending method [19] and the alternating direction method of multipliers (ADMM) [20] overcomes the drawbacks of the original domain solution method [21]-[23]. Some documents apply ADMM to the study of coordinated regulation of integrated energy systems [24] to solve the problem of opaque information between different energy types.

In summary, in the current research on integrated energy coordination and control methods, centralized control methods are still the mainstay, which has laid a solid foundation for the development of comprehensive energy system control research. The hierarchical control method has higher applicability when balancing the interests of multiple entities, but like the centralized control method, it has the disadvantage of not being able to meet the needs of information privacy among energy subjects. Distributed control methods have gained more application in the field of power systems, which can adapt to the characteristics of multi-agent coupling interaction.

2. The Model Framework

2.1. Distributed Operation Method Based on ADMM

Combining the basic form and iterative principle of the ADMM algorithm to build a cross-regional IES distributed control framework. As shown in Fig.1.

The interaction between multiple energy regions in the outer layer is connected by power lines and natural gas pipelines, taking into account the incomplete information conditions between regions. The internal power system and natural gas system in each area of the inner layer interact, and it is considered that the internal information of the area is shared. To apply the ADMM algorithm to solve the above-mentioned

distributed coordination control problem of the energy system, the system structure needs to be decomposed. Since multiple energy regions are involved, the objective function of each energy region can be regarded as the decomposition of the total objective function, so the ADMM framework can be constructed in combination with the principle of decentralization and consistency. Specifically, the objective function is decomposed as follows.

$$F(\boldsymbol{x}) = \sum_{i=1}^{N} f_i(\boldsymbol{x}_i) \tag{1}$$

where N is the number of energy sub-regions, $\boldsymbol{x}_i \in \boldsymbol{x}$ represents the optimized variable of energy sub-region i, f_i is the corresponding sub-objective function.

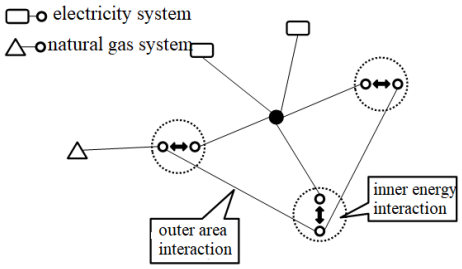

Fig. 1. Distributed coordination control framework.

Therefore, the optimization problem can be decomposed into the sum of each sub-objective function and penalty function, thereby constructing the global consistency problem as follows:

$$\begin{aligned} &\min \ \sum_{i=1}^{N} f_i(\boldsymbol{x}_i) + G(\boldsymbol{z}) \\ &s.t. \ \ \boldsymbol{x}_i - \tilde{\boldsymbol{z}}_i = 0, \ i = 1,2,...,\mathrm{N} \end{aligned} \tag{2}$$

where $\boldsymbol{x}_i$ and $\boldsymbol{z}$ are respectively local optimized variables and global optimized variables, $\boldsymbol{z}$ represents the corresponding component of the global variable in each subregion.

The corresponding Lagrangian function can be expressed as follows:

$$L_\rho(\boldsymbol{x},\boldsymbol{z},\boldsymbol{y}) = \sum_{i=1}^{N}\left[f_i(\boldsymbol{x}_i) + \boldsymbol{y}_i^T(\boldsymbol{x}_i - \tilde{\boldsymbol{z}}_i) + (\rho/2)\left\|\boldsymbol{x}_i - \tilde{\boldsymbol{z}}_i\right\|_2^2 \right] \tag{3}$$

$$\boldsymbol{x}_i^{k+1} = \arg\min_{\boldsymbol{x}_i}\left(f_i(\boldsymbol{x}_i) + \boldsymbol{y}_i^{kT}\boldsymbol{x}_i + (\rho/2)\left\|\boldsymbol{x}_i - \tilde{\boldsymbol{z}}_i^k\right\|_2^2 \right) \tag{4}$$

$$\boldsymbol{z}_g^{k+1} = (1/k_g)\sum_{\Lambda(i)=g} \boldsymbol{x}_i^{k+1} \tag{5}$$

$$\boldsymbol{y}_i^{k+1} = \boldsymbol{y}_i^k + \rho\left(\boldsymbol{x}_i^{k+1} - \tilde{\boldsymbol{z}}_i^{k+1}\right) \tag{6}$$

where k_g represents the number of $\boldsymbol{x}_i$ associated with $\boldsymbol{z}_g$, $\Lambda(i) = g$ represents the mapping from $\boldsymbol{x}_i$ to $\boldsymbol{z}_g$.

Based on the above-mentioned ADMM global consistency framework, the system structure is decomposed. In the outer structure, the distribution of energy resources between different energy regions is realized through power connection lines and connection pipelines. Therefore, the information on the connection lines, pipelines and nodes at both ends is the boundary coupling information.

In the decentralized consistency optimization problem, the iterative update value is a necessary condition for the convergence of the iterative process. The iterative process based on ADMM is that the updated values of the original residual and the dual residual meet the given accuracy requirements:

$$\begin{cases} \left\|\boldsymbol{r}^k\right\|_2 = \left\|\boldsymbol{x}^k - \boldsymbol{z}^k\right\|_2 \le \varphi^{pri} \\ \left\|\boldsymbol{s}^k\right\|_2 = \left\|\lambda\left(\boldsymbol{z}^k - \boldsymbol{z}^{k-1}\right)\right\|_2 \le \varphi^{dual} \end{cases} \tag{7}$$

where $\boldsymbol{r}$ and $\boldsymbol{s}$ are the original residual and the dual residual, φ^{pri} and φ^{dual} are the accuracy requirements of the given original residual and dual residual.

Considering the sensitivity of the ADMM algorithm's convergence speed to the penalty parameter ρ, the following method of varying the penalty parameter is used to speed up the convergence speed of each iteration:

$$\rho^{k+1}=\begin{cases}\rho^{k}\left(1+\eta^{incr}\right) & \textbf{\textit{if}}\ \ \left\|\boldsymbol{r}^{k+1}\right\|>\mu^{incr}\left\|\boldsymbol{s}^{k+1}\right\| \\ \rho^{k}\left(1+\eta^{decr}\right)^{-1} & \textbf{\textit{if}}\ \ \left\|\boldsymbol{s}^{k+1}\right\|>\mu^{decr}\left\|\boldsymbol{r}^{k+1}\right\| \\ \rho^{k+1} & \textbf{\textit{otherwise}}\end{cases} \tag{8}$$

The corresponding program implementation process can be summarized as the following steps:

Step 1: Basic parameter setting. Set the basic parameters and decision variables of each energy zone, set the basic parameters and node information of the tie line between the zones, set the optimization time constant and the upper limit of the number of iterations;

Step 2: Assign initial value. Set the boundary coupling variables between regions and their initial values, including two types of local variables of coupling node voltage and air pressure and corresponding global variables, set the initial values of dual variables and penalty parameters, and set the initial values of the number of iterations;

Step 3: Optimize the calculation. Construct the Lagrangian function in the form of formula for each area, and list other various constraints to perform optimization calculations, and then exchange the coupling variable information to update global variables;

Step 4: Update the multiplier and penalty terms.

Step 5: Determine whether to converge. Calculate the original residual and dual parameters and determine whether the convergence condition is met; if the convergence condition is met, exit the loop and go to step 7;

Step 6: Determine whether it exceeds the iteration requirements. Update the number of iterations and compare it with the upper limit of the number of iterations. If the current number of iterations exceeds the upper limit, exit the loop and prompt that no feasible solution is found;

Step 7: Output the result. Output and save data such as unit output, node status information, boundary coupling node information, and objective function value of each energy zone in each period.

2.2. Optimal Dispatch Constrains

In cross-border energy transactions, the power transaction objects are still mainly wind power and other renewable energy power generation transactions. When the wind power consumption capacity in the region is insufficient, power transmission is an important way to reduce the penalty cost of wind abandonment. In the case of power trans-regional transaction costs, regions with surplus wind power are driven to conduct trans-regional power transactions. There is a strong supply-demand relationship in natural gas cross-border transactions, that is, the natural gas receiver must purchase natural gas from the supplier to meet local demand. This is a safety constraint and is not affected by the optimization goal. Therefore, cross-border natural gas transaction costs may not be considered. For any energy region, the objective function can be expressed in the following form:

$$\begin{aligned}\min\ f_i=&\sum_{t\in T}\left[\sum_{r\in N_r}C_r^{tu}P_{r,t}^{tu}+\sum_{s\in N_s}C_s^{wl}f_{s,t}^{wl}\right]\\&+\sum_{t\in T}\left[\sum_{k\in N_k}C_k^{cut}P_{k,t}^{cut}+\sum_{e\in N_e}C_e^{p2g}f_{e,t}^{p2g}\right]\end{aligned} \tag{9}$$

In addition to the objective function, various system parameters need to meet safety constraints during the optimization and control process. The overall system is divided into three parts: power system constraints, natural gas system constraints, and coupled system constraints.

(1) Power system constraints

$$\begin{cases}P_i=U_i\sum_{j\in i}U_j\left(G_{ij}\cos\theta_{ij}+B_{ij}\sin\theta_{ij}\right)\\Q_i=U_i\sum_{j\in i}U_j\left(G_{ij}\sin\theta_{ij}-B_{ij}\cos\theta_{ij}\right)\end{cases}$$

where P_i and Q_i are the active and reactive power injected into node i, U_i are the voltage amplitude of node i, θ_{ij} is the voltage phase angle difference between node i and j, G_{ij} and B_{ij} the conductance and susceptance of branch ij.

$$\begin{cases}\sum_{k\in i}P_{k,t}^{wu}+\sum_{r\in i}P_{r,t}^{tu}+\sum_{h\in i}P_{h,t}^{gu}=P_{i,t}^{a}+P_{i,t}^{load}+\sum_{l\in i}\omega P_{l,t}^{d}+\sum_{e\in i}P_{e,t}^{p2g}\\ \sum_{k\in i}Q_{k,t}^{wu}+\sum_{r\in i}Q_{r,t}^{tu}+\sum_{h\in i}Q_{h,t}^{gu}=Q_{i,t}^{a}+Q_{i,t}^{load}+\sum_{l\in i}|\omega|Q_{v,t}^{d}\end{cases} \tag{10}$$

where $P_{h,t}^{gu}$ is the active output of gas turbine; $Q_{k,t}^{wu}$, $Q_{r,t}^{tu}$ and $Q_{h,t}^{gu}$ are the reactive power output of wind turbines, conventional turbines and gas turbines; $P_{i,t}^{load}$ and $Q_{i,t}^{load}$ are node active power and reactive power load; $P_{i,t}^{a}$ and $Q_{i,t}^{a}$ are the active and reactive power injected into node *i*.

In addition, the inequality constraints include various unit output constraints, climbing constraints, node voltage safety constraints, and branch power flow constraints:

$$\begin{cases}\begin{cases}P_u^{\min}\le P_{u,t}\le P_u^{\max}\\ Q_u^{\min}\le Q_{u,t}\le Q_u^{\max}\end{cases}\\ \begin{cases}-\Delta P_u^{down}\le P_{u,t}-P_{u,t-1}\le \Delta P_u^{up}\\ -\Delta Q_u^{down}\le Q_{u,t}-Q_{u,t-1}\le \Delta Q_u^{up}\end{cases}\end{cases} \tag{11}$$

$$\begin{cases}U_i^{\min}\le U_i\le U_i^{\max}\\ \begin{cases}P_{ij}^{\min}\le P_{ij}\le P_{ij}^{\max}\\ Q_{ij}^{\min}\le Q_{ij}\le Q_{ij}^{\max}\end{cases}\end{cases} \tag{12}$$

where $P_{u,t}$ and $Q_{u,t}$ represent the output matrix of various types of units,; $P_u^{\max}$, $P_u^{\min}$, $Q_u^{\max}$ and $Q_u^{\min}$ represent the upper and lower bound matrices of the active and reactive power output of various units; ΔP_u^{up}, ΔP_u^{down}, ΔQ_u^{up} and ΔQ_u^{down} represent the upper and lower bound matrices of the active and reactive power output of each unit in adjacent periods; U_i, $U_i^{\max}$ and $U_i^{\min}$ are the voltage amplitude of node upper and lower limits; $P_{ij}^{\max}$, $P_{ij}^{\min}$, $Q_{ij}^{\max}$ and $Q_{ij}^{\min}$ are the upper and lower limits of the active and reactive power flow of the branch.

(2) Natural gas system constraints

$$f=C_pED^{2.53}\left(\frac{p_j^2-p_k^2}{Z\rho_0^{0.96}\mathrm{TL}}\right)^{0.51} \tag{13}$$

where C_p is the transmission coefficient of the pipeline; E is the gas transmission efficiency of the pipeline, and the value is related to the roughness of the pipe wall. Generally, it is in the range of 0.9 to 0.96.

$$\frac{f_k-f_j}{L}+\frac{\pi}{4}\frac{D^2}{R_a\mathrm{T}Z\rho_0}\frac{\tilde{p}_{jk}-\tilde{p}_{jk,t-\Delta t}}{\Delta t}=0 \tag{14}$$

$$f_{jk}=\frac{1}{2}(f_j+f_k) \tag{15}$$

where f_j and f_k is the gas flow in and out of pipeline *jk*, f_{jk} is the average gas flow of pipeline *jk*, p_{jk} is the average gas pressure of pipeline *jk*.

$$V_{jk}-V_{jk,t-\Delta t}=\left(f_j-f_k\right)\Delta t \tag{16}$$

$$V_{jk}=\frac{\pi}{4}\frac{D^2L}{R_a\mathrm{T}Z\rho_0}\tilde{p}_{jk} \tag{17}$$

The gas turbine unit and power to gas unit consumption equation can be expressed as:

$$\begin{cases}H=\alpha+\beta P^{gu}+\gamma\left(P^{gu}\right)^2\\ f^{gu}=H\ /G_v\end{cases} \tag{18}$$

$$f^{p2g}=\eta P^{p2g} \tag{19}$$

where H is the heat input to the gas turbine unit; α, β and γ are the heat consumption coefficient of the gas turbine unit; G_v is the high calorific value of natural gas, the value is 39.84 MJ/Nm3; P^{p2g} is the electrical power input to the P2G device; f^{p2g} is the corresponding gas production; η is the conversion factor.

The raw material cost of P2G equipment includes the cost of water and carbon dioxide consumption. The raw material cost coefficient is calculated as follows:

$$C^{p2g}=\alpha_{\mathrm{H_2O}}C_{\mathrm{H_2O}}+\alpha_{\mathrm{CO_2}}C_{\mathrm{CO_2}} \tag{20}$$

where C^{p2g} is the P2G equipment raw material cost coefficient, C_{H_2O} and C_{CO_2} are the acquisition cost coefficient for water and carbon dioxide, α_{H_2O} and α_{CO_2} are the water and carbon dioxide coefficients required for P2G equipment to produce a unit volume of gas.

At the same time, the natural gas network satisfies the node gas flow balance constraints and the constraints on the gas source gas supply, the node gas pressure, and the initial and final pipe inventory:

$$\begin{cases} \sum_{s\in j} f_{s,t}^{wl} + \sum_{k\in j}\left(f_{jk,t}^{in} - f_{jk,t}^{out}\right) + \sum_{e\in j} f_{e,t}^{p2g} = f_{j,t}^{load} + \sum_{c\in j} \chi_c f_c^{in} + \sum_{h\in j} f_{h,t}^{gu} \\ f_s^{wl,\min} \le f_{s,t}^{wl} \le f_s^{wl,\max} \\ p_j^{\min} \le p_j \le p_j^{\max} \\ \sum_{jk\in N_m} V_{jk,1} - \upsilon \le \sum_{jk\in N_m} V_{jk,T} \le \sum_{jk\in N_m} V_{jk,1} + \upsilon \end{cases} \tag{21}$$

where $f_{jk,t}^{in}$ and $f_{jk,t}^{out}$ are the gas flow into and out of node j, $f_{j,t}^{load}$ is the natural gas load at node j, $f_{h,t}^{gu}$ is the gas consumption of the gas turbine unit, $f_s^{wl,\max}$ and $f_s^{wl,\min}$ are the upper and lower limits of the gas supply in each period of time, $p_j^{\max}$ and $p_j^{\min}$ are the upper and lower pressure limits of node j, υ is the change limit of the line pack during the beginning and end of the management period.

3. Case Study

Considering the complexity of the established cross-region IES distributed coordination control model, a two-region 12bus-12node simple test case is used to verify the feasibility, convergence and solution of the algorithm. The system simulation program is written on MATLAB 2019a software, and the CPLEX solver is called to solve it. The key coefficient settings of the ADMM iteration process are shown in Table I:

TABLE I. KEY COEFFICIENT SETTINGS OF ADMM

η^{incr}	η^{decr}	μ^{incr}	μ^{decr}	φ^{pri}	φ^{dual}
1	1	10	10	0.001	0.001

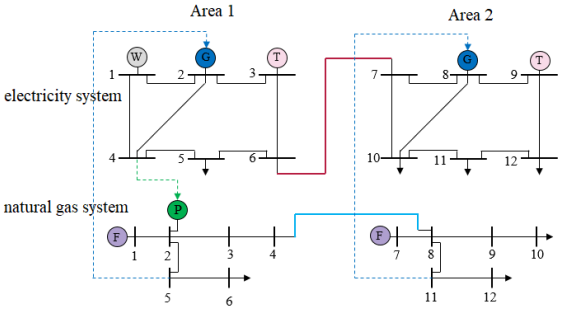

Fig. 2.Two-region 12bus-12node case structure.

To analyze the specific effect of the variable penalty parameter update method used on the convergence of the ADMM algorithm, the penalty parameter is unchanged during the iteration process (set to constant coefficient 1) and the variable penalty parameter is iteratively solved respectively. The initial values of the penalty parameters and boundary coupling variables are set to the same value in this iterative mode. The convergence process of the original residual and the dual residual is shown in Fig.3, and the key data such as the number of iterations and calculation time are shown in Table II.

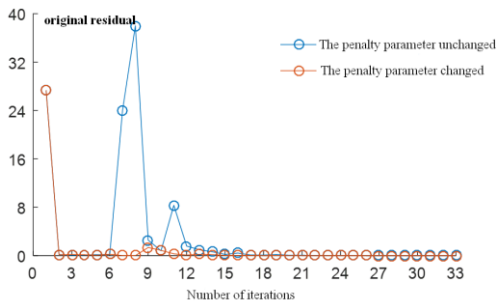

(a) Convergence of the original residual

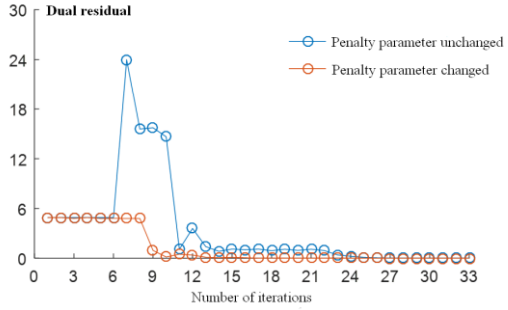

(b) Dual residual convergence process

Fig. 3. Convergence process of original residual and dual residual.

TABLE II. KEY DATA OF THE ITERATIVE PROCESS

	Number of shocks	Number of iterations	Solution time/sec
Penalty parameter unchanged	18	33	122.6
Penalty parameter changed	9	26	97.3

It can be seen from Fig.3 that in the first 6 iterations, the values of the original residual and the dual residual of the two iteration methods are approximately the same. The residual values are relatively large, because the initial values of the boundary coupling variables are all set to 1. There is a big difference between the value of the final optimization result. In the 6th to 12th iterations, when using the update method with the penalty parameter unchanged, both the original residual and the dual residual have obvious fluctuations. The reason for the residual fluctuation is related to the characteristics of the augmented Lagrangian relaxation algorithm. Combined with the number of oscillations in Table, it can be seen that the update method of changing the penalty parameter can effectively reduce the fluctuation range and number of the residual. After the 12th iteration, the residual error has been reduced to a lower level under the two methods, and although there is still a shock, the fluctuation range is small. Finally, the two iteration methods meet the convergence conditions after the 33rd and 26th iterations respectively. Since whether the variable penalty parameter method is adopted will not affect the respective solution process in each iteration area, in terms of the total solution time, the reduced solution time of the variable penalty parameter method is closely related to the reduced number of iterations.

To analyze the convergence of the two residuals, the changes of the original residuals and the dual residuals under the variable penalty parameter mode are compared and analyzed, as shown in Fig.4. The residual of the first iteration is ignored here, because it is affected by the initial value setting and causes a large deviation. It can be seen that the original residual calculation is the deviation of each subject's boundary coupling variable from the global variable, which can represent the subjective willingness of each subject in each iteration of the calculation. It can be seen from Fig.4 that in the first 8 iterations, the value of the original residual is significantly smaller than the dual residual, indicating that the optimal individual benefits between the two regions cannot meet the global optimal condition. So, the operating state must be changed. But in order not to sacrifice individual interests, the operating status has not undergone a substantial change. Until the conditions are really not met, from the 9th to 14th iterations, the individual interests are sacrificed to seek the global optimal solution.

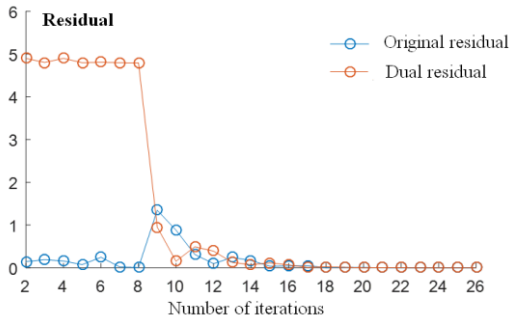

Fig. 4 Change the penalty parameter residual comparison.

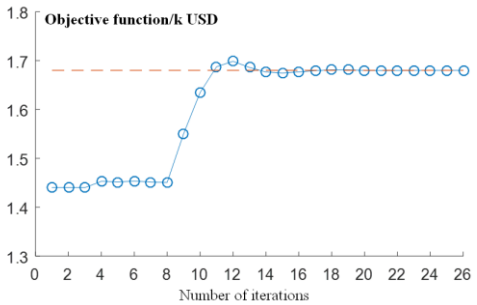

Fig. 5 Change of objective function.

From Fig.5, it can be seen that the global objective function is slow during the first 8 iterations. Changes began to be achieved during the 9th to 14th iterations and gradually tended to the global optimum. After the 15th iteration of the iterative process, the residual has been basically less than 0.1, and the iteration gradually approaches the optimal solution.

The result comparison is shown in Table III. It can be seen that, without considering the cost and benefits of inter-regional energy transactions after decomposition, and the convergence criterion is sufficiently small, the optimization results of distributed control operation and unified centralized control are basically the same in all aspects, but from the perspective of solution time, The calculation time of distributed control is nearly ten times slower than that of centralized control. The reason is that the distributed control framework based on ADMM is essentially a large cyclic framework. Each subject needs to constantly exchange coupling variable information and iteratively seek global optimal solutions.

TABLE III. COMPARISON OF DISTRIBUTED AND CENTRALIZED CONTROL RESULTS

	Electricity trading /MW	Gas trading/km^3	P2G/MW	Operating costs/k USD	Solution time/sec
centralized	18.091	33.752	21.465	1.680	9.6
distribute	18.091	33.752	21.465	1.680	97.3

4. Acknowledgements

This work was supported by a grant from the science and technology program of Global Energy Interconnection Group Co., Ltd (No. SGGEIG00HZJS2100034), the Research on flexibility modeling and collaborative optimization decision-making technology of regional integrated energy supply system based on global energy interconnection.

5. References

[1] G Pan Z, Guo Q, Sun H. Interactions of District Electricity and Heating Systems Considering Time-Scale Characteristics Based on Quasi-Steady Multi-Energy Flow[J]. *Appl. Energy*, 2016, 167: 230–243.

[2] Jia Hongjie. Research on some key problems related to integrated energy systems[J]. *Auto. Elec Power Syst*, 2015, 39(07): 198-207.

[3] D. Wang, "Integrated energy efficiency evaluation of a multi-source multi-load desalination micro-energy network", Global Energy Interconnection, vol. 3, no. 3, pp. 128-139, 2020.

[4] Y. Zhao, , "Flexibility Evaluation Method of Power System Considering the Impact of Multi-Energy Coupling," in IEEE Trans. Industry Applications, vol. 57, no. 6, pp. 5687-5697, Nov.-Dec. 2021.

[5] Xu Xiandong. Study on Hybrid Heat-Gas-Power Flow Algorithm for Integrated Community Energy System[J]. Proceedings of the Chinese Society of Electrical Engineering, 2015, 35(14): 3634-3642.

[6] Chen Sheng. Probabilistic Energy Flow Analysis in Integrated Electricity and Natural-gas Energy systems[J]. Proceedings of the Chinese Society of Electrical Engineering, 2015, 35(24): 6331-6340.

[7] Carlos M, Correa-Posada, Pedro Sánchez-Martín. Integrated Power and Natural Gas Model for Energy Adequacy in Short-Term Operation[J]. *IEEE Trans. Power Syst*, 2015, 30(6): 3347-3355.

[8] Wang Y, Wang Y, Huang Y, et al. Operation optimization of regional integrated energy system based on the modeling of electricity-thermal-natural gas network[J]. *Appl. Energy*,2019,251: 1-27.

[9] Hao Ran. Hierarchical optimal dispatch based on energy hub for regional integrated energy system[J]. Electric Power Automation Equipment, 2017, 37(06): 171-178.

[10] Su Xiaolin. Hierarchical Coordinated Control System of Active Distribution Network and Its Regional Autonomy Strategy[J]. *Auto. Elec Power Syst*, 2017, 41(06): 129-134+141.

[11] Z. Zhang, "Day-Ahead Optimal Dispatch for Integrated Energy System Considering Power-to-Gas and Dynamic Pipeline Networks," in *IEEE Trans. Industry App*, vol. 57, no. 4, pp. 3317-3328, July-Aug. 2021.

[12] Xu Yutian. Bi-level Integrated Energy Planning Method Considering Active Management Measures in Electricity Market Environment[J]. *Auto. Elec Power Syst*, 2018, 42(18): 114-122.

[13] Z. Zhang, "Multi-time Scale Co-optimization Scheduling of Integrated Energy System for Uncertainty Balancing," *I&CPS Asia*, 2021, pp. 270-276.

[14] YANG Jingwei, ZAHNG Ning, KANG Chongqing, et al. A State-Independent Linear Power Flow Model with Accurate Estimation of Voltage Magnitude[J]. *IEEE Trans. Power Syst*, 2017, 32(5): 3607-3617.

[15] F. Liu, C. Wang, Z. Zhang, H. Lv and M. Zhang, "Decentralized Economic Dispatch of Integrated Electricity-gas Energy System Considering P2G and Line Pack," *EI*^{2}, 2020, pp. 267-272.

[16] Y. Zhao, J. Yu, M. Ban, Y. Liu and Z. Li, "Privacy-Preserving Economic Dispatch for An Active Distribution Network with Multiple Networked Microgrids", *IEEE Access*, vol. 6, pp. 38802-38819, 2018.

[17] Xingxu Zhu. A Distributed Algorithm for Time-varying Optimal Power Flow Tracking in Distribution Networks With Photovoltaics and Energy Storage[J]. Proceedings of the Chinese Society of Electrical Engineering, 2019,

39(09): 2644-2658.

[18] Duchi J C, Agarwal A. Dual Averaging for Distributed Optimization: Convergence Analysis and Network Scaling[J]. IEEE Transactions on Automatic Control, 2012, 57(3): 592-606.

[19] Gower R M, Richtarik P. Stochastic Dual Ascent for Solving Linear Systems[J]. Mathematics, 2015: 674-683.

[20] Boyd. Distributed optimization and statistical learning via the alternating direction method of multipliers[M]. Found Trends Mach Learn 2011.

[21] Chen Sheng. Distributed Bilinear State Estimation Based on Alternating Direction Method of Multipliers[J]. *Auto. Elec Power Syst*, 2015, 39(20): 84-90.

[22] Sleiman M. Chapman Adaptive ADMM for Distributed AC Optimal Power Flow[J]. *IEEE Trans. Power Syst*, 2019, 34(3): 2025-2035..

[23] Deeb N I. Cross decomposition for multi-area optimal reactive power planning[J]. *IEEE Trans. Power Syst*, 1993, 8(4): 1539-1544.

[24] M. Sleiman. "Adaptive ADMM for Distributed AC Optimal Power Flow", IEEE Trans. Power Syst, vol. 34, no. 3, pp. 2025-2035